Passivity of AISI 316L Stainless Steel as a Function of Nitric Concentration

A. Fattah-alhosseini[a,*], M. A. Sonamia[a], A. Loghmani[a], F. Zerafati Shoja[a]

[a] *Department of Engineering, Bu-Ali Sina University, Hamedan, Iran.*

ARTICLE INFO

Article history:

Received 11 Feb. 2014
Accepted 09 Mar. 2014
Available online 15 May 2014

Keywords:

EIS
p-type semiconductor
N-type semiconductor
Mott–Schottky

ABSTRACT

In this study, electrochemical behavior of passive films formed on AISI 316L stainless steel (AISI 316L) in three acidic solution concentrations (0.3, 0.6, and 0.9M HNO_3) under open-circuit potential conditions was evaluated by potentiodynamic polarization, Mott–Schottky analysis, and electrochemical impedance spectroscopy (EIS) techniques. The potentiodynamic polarization results showed that the corrosion potentials of AISI 316L shift towards positive direction with increase in solution concentration. Also, these results revealed that the corrosion rate of AISI 316L is enhanced in solutions with higher nitric content. Mott–Schottky analysis revealed that passive films behave as p-type and n-type semiconductors at potentials below and above the flat band potential, respectively. Also, Mott–Schottky analysis indicated that the donor and acceptor densities increased with solution concentration. EIS data showed that the equivalent circuit $R_s((R_{ct}Q_{dl})(R_fQ_f))$ by two time constants is applicable. Moreover, EIS results revealed that charge transfer resistance and passive film resistance decrease with solution concentration.

1. Introduction

AISI 316L stainless steel is used extensively in chemical and petroleum industries because of its good compromise between corrosion resistance, mechanical properties, and economic advantages. Generally, the higher corrosion resistance of stainless steel is due to the presence of passive films formed on the surface. The passive films of metals are mainly made up of metallic oxides or hydroxides which are envisaged as semiconductors. Consequently, semiconducting properties are often observed on the surfaces of the passive metals [1-4].

Mott–Schottky analysis has been extensively used to study the semiconducting properties of passive films, such as the those formed on steels and stainless steels. Passivity of stainless steel is usually attributed to the formation on the metal surface of a mixture of iron and chromium oxide film with semiconducting behavior [5].

It is well known that an increase in solution concentration has significantly detrimental effects on the corrosion properties of stainless steels. Ningshen et al. [6] reported that

Corresponding author:
E-mail address: a.fattah@basu.ac.ir (Arash Fattah-Alhosseini).

concentration has a significant effect on the corrosion resistance of the passive film formed on three indigenous nitric acid grade (NAG) type 304L stainless steel (SS), and two commercial NAG SS designated as Uranus-16 similar to 304L composition and Uranus-65 similar to type 310L SS in 6 N and 11.5 N HNO_3 media. The results in 6 N HNO_3 show that the indigenous NAG 304L SS and Uranus-65 alloy exhibited similar and higher corrosion resistance with lower passive current density compared to Uranus-16 alloy. In higher concentration of 11.5 N HNO_3, transpassive potential of all the NAG SS shows a similar range, except for Uranus-16 alloy [6].

In another study by Ningshen et al. [7], the potentiodynamic anodic polarization results revealed no significant change in the corrosion potential even with increase in nitric acid concentration in the presence of oxidizing ions. Also, in this study, the passive film stability measured by EIS revealed faster passive film dissolution as indicated by low film polarization resistance, with increase in nitric acid concentration [7].

For 304L stainless steel in nitric acid medium, Padhy et al. [8] found that passive film consists of platelet-like structures with a moire´ pattern at lower concentrations (0.1, 0.5 M); at higher concentrations (0.6, 1 M), the platelet-like structures disappear, revealing the grain boundary structure. Also, Padhy et al. [9] found that variation in passive film morphology occurs depending upon the concentration and the time of immersion. In situ surface morphological investigation showed formation of platelet-like structures at lower concentrations (0.1 M, 0.5 M), and towards higher concentration (0.6 M, 1M) the platelet-like structures got agglomerated, homogenized and started depleting from the surface leading to opening up of oxide boundaries. Compositional analysis of the passive film revealed duplex nature at lower concentration consisting of hydroxide and oxide layer, and with increasing concentration the oxide layer predominates over the surface [9].

As mentioned above, the change in the composition and structure of the passive film was found to be responsible for the variation in the corrosion resistance of stainless steels. Moreover, the explanation on these phenomena in terms of the electronic properties of the passive film has remained obscure. The aim of this study was to investigate the influence of solution concentration on the electrochemical behavior of AISI 316L using the potentiodynamic polarization and Mott-Schottky analysis and EIS techniques.

2. Experimental

2. 1. Material and solutions

Specimens were fabricated from AISI 316L with the chemical composition (%, wt.): 17.5 Cr, 13.4 Ni, 2.32 Mo, 1.4 Mn, 0.47 Si, 0.03 P, 0.003 S, 0.03 C. All samples were polished up to 1200 grit and mounted by cold curing epoxy resin. The samples were then degreased with acetone, rinsed in distilled water and dried with air just before each test. Aerated nitric acidic solutions with three different concentrations (0.3, 0.6, and 0.9M HNO_3) were used as the test solutions. All solutions were made from analytical grade of nitric acid mixed with water. Tests were carried out at 25±1 ◦C.

2. 2. Electrochemical measurements

Electrochemical measurements were performed in a conventional three-electrode cell under aerated conditions. The counter electrode was a Pt plate, while the reference electrode was Ag/AgCl saturated in KCl. Electrochemical measurements were obtained by using an Autolab potentiostat/galvanostat system.

Prior to the electrochemical measurements, working electrodes were immersed at OCP for 900 seconds to form a steady-state passive film. Potentiodynamic polarization curves were measured potentiodynamically at a scan rate of 1 mV/s starting from -0.25 $V_{Ag/AgCl}$ (vs. E_{corr}) to 1.1 $V_{Ag/AgCl}$. The impedance spectra were measured in a frequency range of 100 kHz –10 mHz at an AC amplitude of 10 mV (rms). The validation of the impedance spectra was performed by checking the linearity condition, i.e. measuring spectra at AC signal amplitudes between 5 and 15 mV (rms). Each electrochemical measurement was repeated at least three times. For the EIS data modeling and curve-fitting method, NOVA impedance software was used. Mott-Schottky analyses

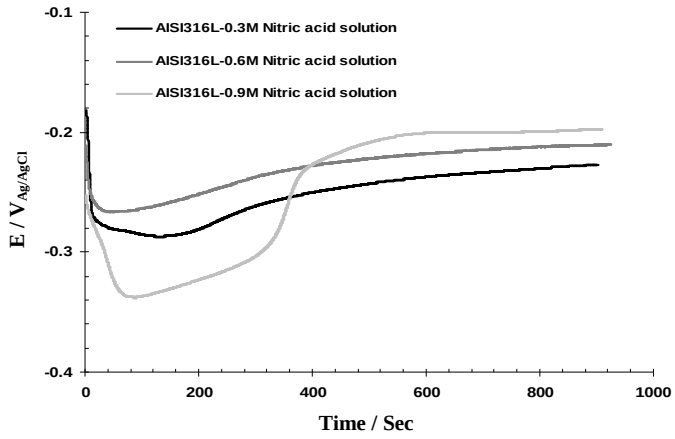

Fig. 1. Open circuit potential plots of AISI 316L in HNO_3 solutions

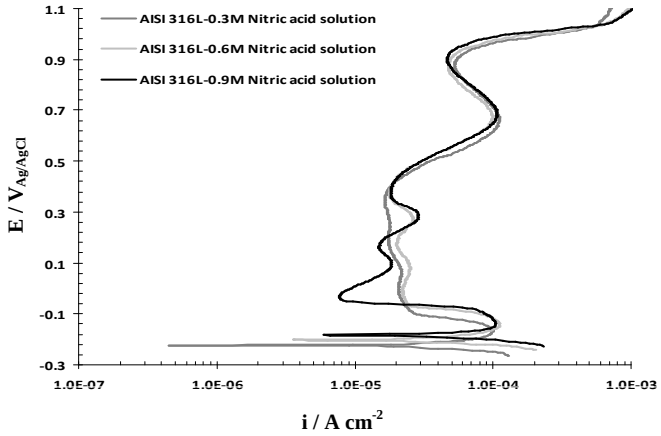

Fig. 2. Potentiodynamic polarization curves for AISI 316L in HNO_3 solutions

were carried out on passive films at a frequency of 1 kHz using a 10 mV ac signal, and a step rate of 25 mV in the cathodic direction.

3. Results and Discussion

3. 1. OCP measurements

In Fig. 1, changes on OCP of AISI 316L in HNO_3 solutions with different concentrations are shown. At the start of immersion, the potential immediately reduces which shows the dissolution of the oxide layer for all solutions. However, as time passes, the open circuit potential is directed towards positive amount. This trend is also reported for austenitic stainless steels in acidic solutions, indicating the formation of passive film and its role in increasing protectivity with time [10]. Fig. 1 also indicates that within 900 seconds, a complete stable condition is achieved and electrochemical tests are possible.

3. 2. Potentiodynamic polarization

Fig. 2 shows the potentiodynamic polarization curves of AISI 316L in HNO_3 solutions with different concentrations. For all concentrations, it is observed that before the electrode surface is transferred to a passive state, an active current peak occurs, which could be related to the oxidation of Fe^{2+} to Fe^{3+} ions in the passive film [11, 12].

The corrosion potential and corrosion current density at different concentrations of HNO_3 solutions for AISI 316L are shown in Fig. 3. The corrosion current density was obtained by Tafel extrapolation method because: (1) the branch of the polarization curve is under activation control, (2) corrosion is uniform (general), (3) there is a well-defined Tafel region, and (4) changes in the electrode potential do not induce additional electrode

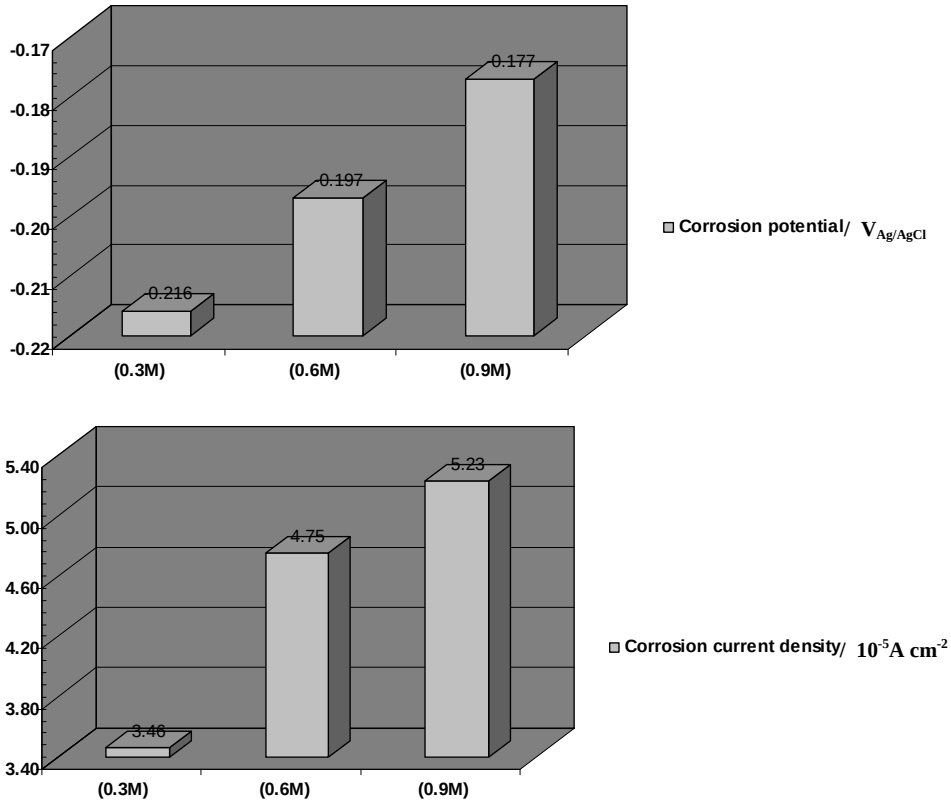

Fig. 3. Corrosion potential and corrosion current density of AISI 316L in HNO_3 solutions

reactions [13]. It is observed from Fig. 3 that the corrosion potentials shift towards positive direction with increase in the solution concentration. Also, the results show that the corrosion current density increases with increase in the concentration of HNO_3 solutions.

3. 3. Mott-Schottky analysis

The corrosion resistance of the passive film was correlated with its semiconducting properties, which could be measured by the Mott–Schottky analysis in high frequency domain. According to the Mott–Schottky analysis, the space charge capacitances of n-type and p-type semiconductor were given by the following Mott–Schottky relationships (1) and (2), assuming that the capacitance of the Helmholtz layer could be neglected [14-16]:

$$\frac{1}{C^2} = \frac{2}{\varepsilon\varepsilon_0 e N_D}\left(E - E_{FB} - \frac{kT}{e}\right) \quad \text{for n-type semiconductor} \quad [1]$$

$$\frac{1}{C^2} = -\frac{2}{\varepsilon\varepsilon_0 e N_A}\left(E - E_{FB} - \frac{kT}{e}\right) \quad \text{for n-type semiconductor} \quad [2]$$

where e is the electron charge, N_D is the donor density for n–type semiconductor (cm^{-3}), N_A is the acceptor density for p–type semiconductor (cm^{-3}), ε is the dielectric constant of the passive film (usually taken as 15.6 [14-16]), ε_0 is the vacuum permittivity, k is the Boltzmann constant, T is the absolute temperature and E_{FB} is the flat band potential.

Fig. 4 shows the Mott-Schottky plots of AISI 316L in HNO_3 solutions. Firstly, it should be noted that for all concentration, capacitances clearly increase with solution concentration. Secondly, there are three potential regions where C^{-2} changes linearly with the electrode potential, which is characteristic of semiconductors. The conductivity type of semiconductor appears obviously according to the slope sign of these curves. In the electrode

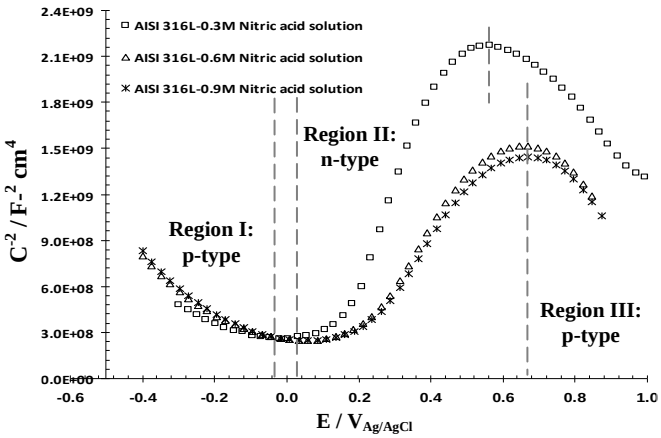

Fig. 4. Mott-Schottky plots of AISI 316L in HNO_3 solutions

potential in region I, the oxide films behave as p-type semiconductors since the slopes are negative.

As it is shown in Fig. 4 and the literature [5, 17-20], the oxide films on stainless steels show Fe enrichment near the outer surface, and Cr enrichment near the metal/oxide interface. The capacitance response below ~ -0.03 $V_{Ag/AgCl}$ can be attributed to the chromium oxides, in which the Cr^{3+} cation vacancies are the main acceptor species and the predominant ionic current carriers. In region II, the oxide films behave as n-type semiconductors due to the positive slopes. The capacitance response can be ascribed to the iron oxides, especially Fe_2O_3, in which Fe^{2+} species or oxygen vacancies are the predominant donors. Finally, the negative slopes in region III are attributed to p-type behavior, with a peak at around 0.67 $V_{Ag/AgCl}$ (except 0.56 $V_{Ag/AgCl}$ for 0.3 M). This feature is usually explained in terms of a strong dependence of the Faradaic current on potential in the transpassive region. In this regard, the behavior of capacitance at high potentials near the transpassive region would be attributed to the development of an inversion layer as a result of increasing concentration in the valence band [17-20].

As can be seen in Fig. 4, there is a potential zone (i.e., from about -0.03 to 0.02 $V_{Ag/AgCl}$) between the p-type and n-type semiconductive regions, where the electronic band structures of the oxide films are in the flat band conditions. The charge transfer in turn governs these positions across the semiconductor/electrolyte interface. Thus, Mott-Schottky analysis shows that the passive films formed on this stainless steel behave as p-type and n-type semiconductors above and below the flat band potential, respectively. This behavior implies that the passive films have a duplex structure, which would not have been realized if the measurements were restricted to only anodic potentials. Early studies of the bipolar duplex structures of passive films on stainless steels were carried out by Sato [21], and followed by Ferreira et al., and Oguzie et al. [22, 23]. It has been well established that the inner part of the passive film, which has a p-type behavior, consists mainly of Cr oxides, while the outer region, with an n-type behavior, predominantly consists of Fe oxides [24].

According to Eq. (1), donor density has been determined from the positive slopes in region II of Fig. 4. Also, the acceptor density has been calculated from the negative slopes in region III of Fig. 4, according to Eq. (2). Fig. 5 shows the calculated donor and acceptor densities for the passive films formed on AISI 316L in HNO_3 solutions. The orders of magnitude are around 10^{21} cm^{-3} and are comparable to those reported in other studies [5]. According to Fig. 5, the donor and acceptor densities increase with solution concentration, respectively. Changes in donor and acceptor densities correspond to the non-stoichiometry defects in the passive film.

3. 4. EIS measurements

Fig. 6 presents bode modulus plots obtained for

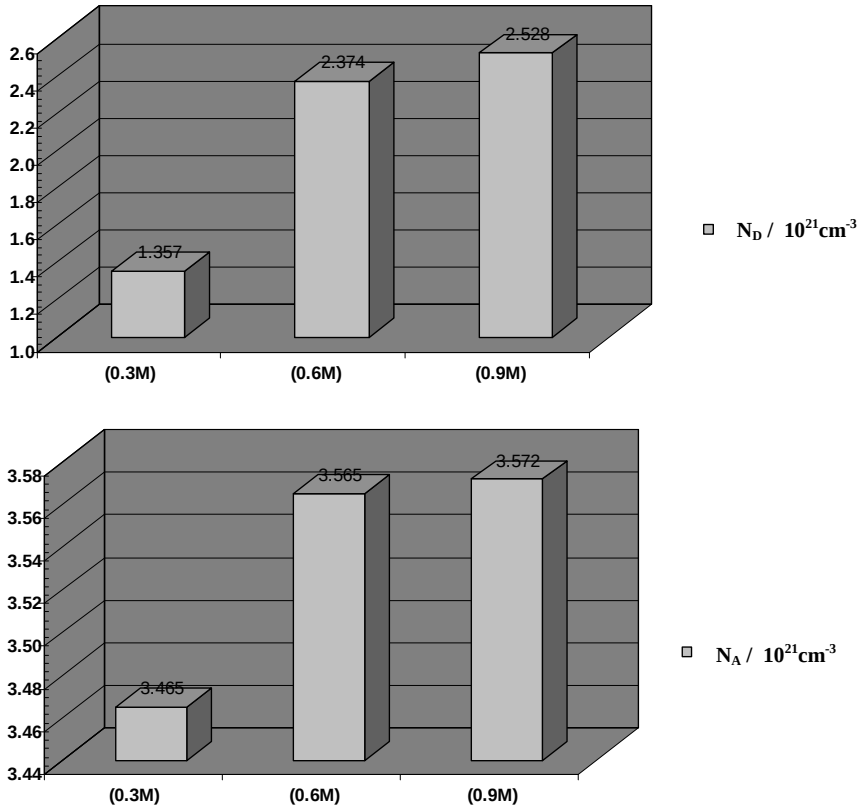

Fig. 5. Donor and acceptor densities of the passive films formed on AISI 316L in nitric acid solutions as a function of concentration

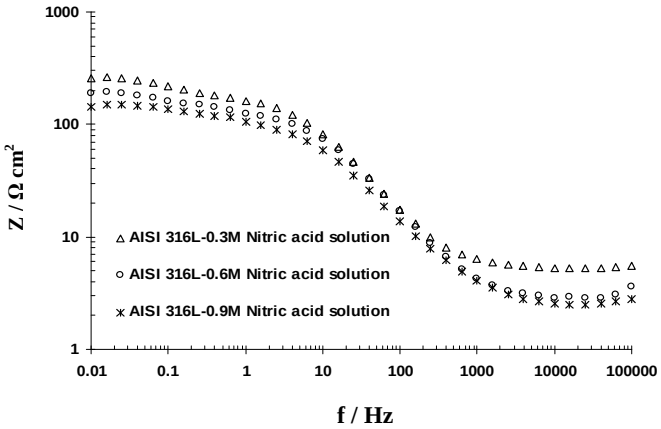

Fig. 6. Bode modulus plots of AISI 316L in HNO_3 solutions

the AISI 316L at OCP after 900 seconds immersion in HNO_3 solutions. As can be seen from Fig. 6, bode modulus plots in three solutions show the same behavior. It should be noted that for three concentration, impedance Z)(clearly decreases with solution concentration.

The equivalent circuit shown in Fig. 7 was used to simulate the measured impedance data on AISI 316L in HNO_3 solutions. This equivalent circuit has been reported as excellent to model the passivation of stainless steels in acidic media [25]. This circuit presents two time constants. The interpretation suggested for the circuit elements is the following one: the high frequencies (R_{ct}: charge transfer resistance, Q_{dl}: double layer constant phase

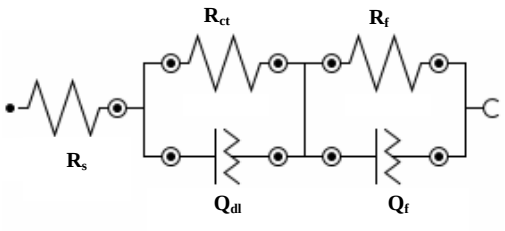

Fig. 7. The best equivalent circuit used to model the experimental EIS data

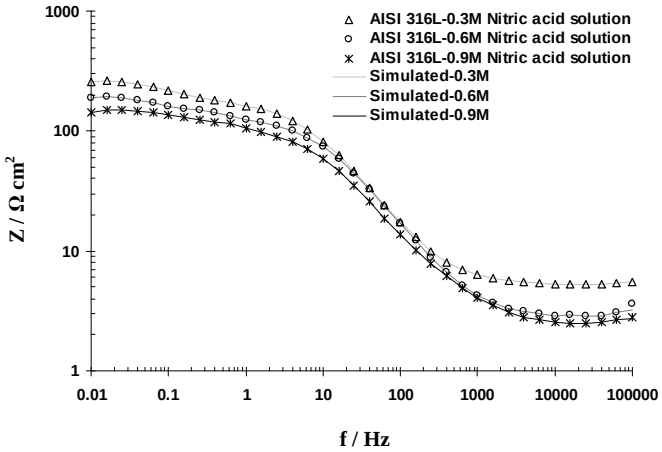

Fig. 8. The fitting results of bode modulus plots of AISI 316L in HNO_3 solutions

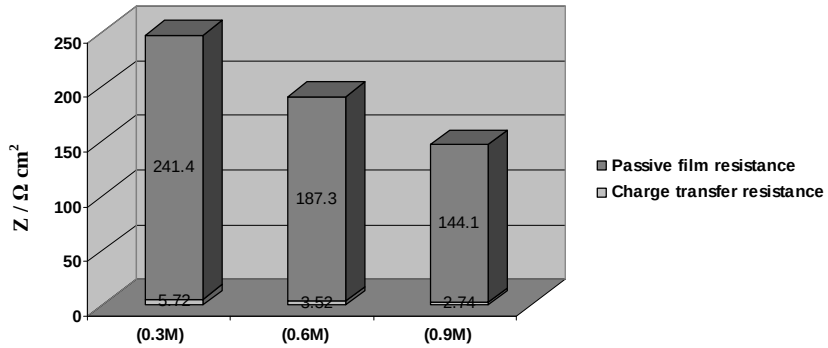

Fig. 9. Passive film resistance and charge transfer resistance of AISI 316L in nitric acid solutions as a function of concentration

element) time constant can be associated with the charge transfer process and the low frequencies (R_f: passive film resistance, Q_f: passive film constant phase element) time constant can be correlated with the passive film formation.

As it is shown in Fig. 8, this equivalent circuit was provided best fitting for the impedance data. Fig. 9 shows the variation of charge transfer resistance and passive film resistance for AISI 316L in 0.3, 0.6 and 0.9M HNO_3 solutions. As can be seen from this figure, the polarization resistance (= R_{ct} + R_f) in three solutions decreases with solution concentration.

4. Conclusions

Semiconducting properties of passive films formed on AISI 316L in HNO_3 solutions were investigated in the present work. Conclusions drawn from the study are as follows

1. The polarization curves suggested that AISI 316L showed excellent passive behavior in nitric

solutions.

2. By comparing the polarization curves in different solution, the corrosion potentials were found to shift towards positive direction with an increase in solution concentration.
3. For all concentrations, it is observed that before the electrode surface is transferred to a passive state an active current peak occurs, which could be related to the oxidation of Fe^{2+} to Fe^{3+} ions in the passive film.
4. Mott–Schottky analysis revealed that the existence of a duplex passive film structure composed of two oxide layers of distinct semiconductivities.
5. Based on the Mott–Schottky analysis, it was shown that donor and acceptor densities are in the range of 10^{21} cm^{-3} and increase with solution concentration.

References

1. Z. Shi G. Song, CN. Cao, H. Lin, M. Lu, "Electrochemical potential noise of 321 stainless steel stressed under constant strain rate testing conditions", Electrochim. Acta., Vol. 52, 2007, pp. 2123–2133.
2. AA. Hermas, MS. Morad, "A comparative study on the corrosion behaviour of 304 austenitic stainless steel in sulfamic and sulfuric acid solutions", Corros. Sci., Vol. 50, 2008, pp. 2710–2717.
3. NE. Hakiki, M. Da Cunha Belo, AMP. Simões, MGS. Ferreira, "Semiconducting properties of passive films on stainless steel. Influence of the alloying elements", J Electrochem. Soc., Vol. 145, 1998, pp. 3821–3289.
4. MC. Li, H. Zhang, RF. Huang, SD. Wang, HY. Bi, "Effect of SO_2 on oxidation of type 409 stainless steel and its implication on condensate corrosion in automotive mufflers", Corros. Sci., Vol. 80, 2014, pp. 96–103.
5. A. Fattah-alhosseini, F. Soltani, F. Shirsalimi, B. Ezadi, N. Attarzadeh, "The semiconducting properties of passive films formed on AISI 316 L and AISI 321 stainless steels: A test of the point defect model (PDM)", Corros. Sci., Vol. 53, 2011, pp. 3186–3192.
6. S. Ningshen, UK. Mudali, G. Amarendra, B. Raj, "Corrosion assessment of nitric acid grade austenitic stainless steels", Corros. Sci., Vol. 51, 2009, pp. 322–329.
7. S. Ningshen, UK. Mudali, G. Amarendra, B. Raj, "Corrosion behaviour of AISI type 304L stainless steel in nitric acid media containing oxidizing species", Corros. Sci., Vol. 53, 2011, pp. 64–70.
8. N. Padhy, S. Ningshen, UK. Mudali, G. Amarendra, B. Raj. "In situ surface investigation of austenitic stainless steel in nitric acid medium using electrochemical atomic force microscopy", Scripta Materialia, Vol. 62, 2010, pp. 45–48.
9. N. Padhy, S. Ningshen, UK. Mudali, G. Amarendra, B. Raj, "Morphological and compositional analysis of passive film on austenitic stainless steel in nitric acid medium", Appl. Surf. Sci., Vol. 257, 2011, pp. 5088–5097.
10. A. Fattah-alhosseini, MM. Khalvan, "Semiconducting properties of passive films formed on AISI 420 stainless steel in nitric acid solutions", J. Advan. Mater. Process., Vol. 2, 2013, pp. 15–22.
11. K. Azumi, T. Ohtsuka, N. Sata, "Mott-Schottky plot of the passive film formed on iron in neutral borate and phosphate solutions", J. Electrochem. Soc., Vol. 134, 1987, pp. 1352–1358.
12. DD. Macdonald, KM. Ismail, E. Sikora "Characterization of the passive state on zinc", J. Electrochem. Soc., Vol. 145, 1998, pp. 3141–3149.
13. E. McCafferty, "Validation of corrosion rates measured by the Tafel extrapolation method", Corros. Sci., Vol. 47, 2005, pp. 3202–3215.
14. H. Luo, XG. Li, CF. Dong, K. Xiao, XQ, Cheng, "Influence of uv light on passive behavior of the 304 stainless steel in acid solution", J. Phys. Chem. Solid., Vol. 74, 2013, pp. 691–697.
15. Y. Yang, LJ. Guo, H. Liu, "Effect of fluoride ions on corrosion behavior of SS316L in simulated proton exchange membrane fuel cell (PEMFC) cathode environments", J. Power Sourc., Vol. 195, 2010, pp. 5651–5659.
16. J. Ding, L. Zhang, M. Lu, J. Wang, Z. Wen, W. Hao, "The electrochemical behaviour of 316L austenitic stainless steel in

Cl^-containing environment under different H_2S partial pressures", Appl. Surf. Sci., Vol. 289, 2014, pp. 33– 41.
17. C. Escrivà-Cerdán, E. Blasco-Tamarit, DM. García-García, J. García-Antóna, A. Guenbour. "Effect of potential formation on the electrochemical behaviour of a highly alloyed austenitic stainless steel in contaminated phosphoric acid at different temperatures", Electrochim. Acta., Vol. 80, 2012, pp. 248–256.
18. DD. Macdonald, "On the existence of our metals-based civilization I. Phase-space analysis", J. Electrochem. Soc. Vol. 153, 2006, pp. B213–B224.
19. DD. Macdonald, "On the tenuous nature of passivity and its role in the isolation of HLNW", J. Nuclear Materials. Vol. 379, 2008, pp. 24–32.
20. A. Fattah-alhosseini, MA. Golozar, A. Saatchi, K. Raeissi, "Effect of solution concentration on semiconducting properties of passive films formed on austenitic stainless steels", Corros. Sci. Vol. 52, 2010, pp. 205-209.
21. N. Sato, "An overview on passivity on metals", Corros. Sci., Vol. 31, 1990, pp. 1–19.
22. MGS. Ferreira, NE. Hakiki, G. Goodlet, S. Faty, AMP. Simões, M. Da Cunha Belo, "Influence of the temperature of film formation on the electronic structure of oxide films formed on 304 stainless steel", Electrochim. Acta., Vol. 46, 2001, pp. 3767–3776.
23. EE. Oguzie, J. Li, Y. Liu, D. Chen, Y. Li, K. Yang, F. Wang, "The effect of Cu addition on the electrochemical corrosion and passivation behavior of stainless steels", Electrochim. Acta., Vol. 55, 2010, pp. 5028–5035.
24. L. Jinlong, L. Hongyun. "Comparison of corrosion properties of passive films formed on phase reversion induced nano/ultrafine-grained 321 stainless steel", Appl. Surf. Sci., Vol. 280, 2013, pp. 124–131.
25. M. Criado, DM. Bastidas, S. Fajardo, A. Fernández-Jiménez, JM. Bastidas, "Corrosion behaviour of a new low-nickel stainless steel embedded in activated fly ash mortars", Cem. Concr. Comp., Vol. 33, 2011, pp. 644–652.